ORIGINAL PAPER

Electrochemical studies with dissolved and surface-confined forms of *neo*-pentyl-ferrocene-based polyesters utilising [NBu$_4$][B(C$_6$F$_5$)$_4$] and other electrolytes

Ayman Nafady · C. John McAdam · Alan M. Bond · Stephen C. Moratti · Jim Simpson

Abstract The voltammetric oxidation at a glassy carbon electrode of a series of ferrocenyl polyesters **PmF{X}**, (**X=T**, terephthalate; **N**, 2,6-naphthalene dicarboxylate; **B**, 4,4′-biphenyl dicarboxylate) is reported in the weakly donating and low-polarity CH$_2$Cl$_2$ solvent containing [NBu$_4$][PF$_6$], [NBu$_4$][B(C$_6$F$_5$)$_4$], or 1-butyl-1-methylpyrrolidinium bis(trifluoromethylsulfonyl)amide ([bmpyr][TFSA]) as the supporting electrolyte. The one electron oxidation of the ferrocenyl groups is strongly influenced by the nature of the supporting electrolyte anion. Use of the conventional [PF$_6$]$^-$ anion or the room temperature ionic liquid (RTIL), [bmpyr][TFSA] as the supporting electrolyte, gives rise to significant oxidation product interaction (precipitation and/or adsorption) with the electrode surface. In marked contrast, diffusion-controlled, chemically and electrochemically reversible processes are observed when the weakly coordinating [B(C$_6$F$_5$)$_4$]$^-$ is used as the anionic component of the supporting electrolyte. In this case, data obtained via cyclic voltammetry, chronoamperometry and chronocoulometry are consistent with ideal reversible one electron oxidation processes and a soluble cationic product. Diffusion coefficients of the monomers, polymers, ferrocene and decamethyferrocene are reported in the CH$_2$Cl$_2$/ [NBu$_4$][B(C$_6$F$_5$)$_4$] system. Importantly, reversible potentials that are easily obtained under these conditions show that the acyl or methyl linkers, through which the ferrocenyl group is attached to the *neo*-pentylenediol component, tune the redox properties of the polymers. Electrochemical studies with a glassy carbon electrode modified with microcrystals of the **PmFT** polymer conducted in aqueous (with KCl supporting electrolyte) or neat ionic liquid ([bmpyr][TFSA]) media also are reported. Different mechanisms apply in each of these cases.

Introduction

The first ferrocene-containing macromolecule, poly(vinylferrocene) made an understated entrance into the chemical literature in 1955 [1]. A decade passed before significant attempts were made to expand the boundaries of metallopolymer science [2], and re-invigoration occurred in the 1990s with new synthetic routes offering higher molecular weights and narrower molecular weight distributions [3]. The driving force for current efforts is the unusual and useful properties that arise from the combination of the redox-active metal centres with the macromolecular polymer component. Incorporation of ferrocene as the organometallic residue offers particular advantages [4]. These include synthetic versatility and good air, moisture and thermal stability, but additionally well-behaved one electron oxidation chemistry and as a consequence, access to the characteristics of the oxidised species. Outputs in this area of research are multidisciplinary [5] and include material science [6], sensing and biomedical applications [7–10].

The two principal architectures of polymeric ferrocenyl materials are side-chain polymers, where the ferrocenyl substituent is attached in some way to the polymer, and main-chain polymers, in which the metallocene is incorporated into the polymer backbone [3, 11]. Detailed electrochemical studies have included both categories [12–17]. In general, solution-phase electrochemistry of ferrocenyl poly-

A. Nafady · A. M. Bond
School of Chemistry, Monash University,
P.O. Box 3800, Clayton, Australia

C. J. McAdam (✉) · S. C. Moratti · J. Simpson
Department of Chemistry, University of Otago,
P.O. Box 56, Dunedin, New Zealand
e-mail: mcadamj@chemistry.otago.ac.nz

mers shows a single Fe^{II}/Fe^{III} redox process suggesting non-interaction between neighbouring sites. The exception to this is when the ferrocenyl redox centres in the polymer are in close proximity, as is found in polyferrocenylsilanes [18]. In this case, cyclic voltammograms display two reversible oxidation processes presumably on account of the electrostatic interaction between the proximal ferrocendiyl centres.

As shown in the work described in this paper, the choice of solvent/supporting electrolyte medium plays a key role in solution-based electrochemical studies of ferrocenyl polymers. Ideally, both the reduced and oxidised forms need to be soluble, whereas marked differences often exist between the solubility of neutral and oxidised polymer species. This problem of poor solubility of the generated oxidation product(s) is highly exacerbated in lower-polarity solvents such as dichloromethane, particularly when traditional counter anions such $[ClO_4]^-$, $[BF_4]^-$ and $[PF_6]^-$ are present in the supporting electrolyte [12]. Pioneering work of the Geiger group has shown that use of an electrochemical medium composed of CH_2Cl_2 and the weakly coordinating *tetrakis*(perfluorophenyl) borate, $[B(C_6F_5)_4]^-$ as the supporting electrolyte anion, may often be superior in improving the solubility and kinetic stability of a variety of cationic species generated via electrochemical oxidation [19–22]. In this context, we have now successfully employed the CH_2Cl_2/0.05 M $[NBu_4][B(C_6F_5)_4]$ medium to circumvent the severe product interaction with a glassy carbon electrode surface observed when $[PF_6]^-$ anion is present, thereby allowing for facile access to redox-based thermodynamic information for the ferrocenyl polyesters. In contrast, the solid-state voltammetric behaviour of **PmFT** (Fig. 1) microcrystals attached to a glassy carbon electrode surface in contact with aqueous 0.1 M KCl electrolyte solution or neat [bmpyr][TFSA] ionic liquid

takes advantage of the poor solubility of the ferrocenyl polyesters and their oxidised forms in these media.

Experimental

The synthesis of the monomers **mF** and **aF** [23] and polymers **PmFT**, **PmFN**, **PmFB** and **PaFT** [24] has been reported elsewhere. Electrochemical measurements were conducted at 293 ± 2 K under a nitrogen atmosphere using a BAS100B computer-controlled electrochemical workstation and a standard three-electrode cell configuration. For voltammetric experiments, glassy carbon disks having either 1.5 mm (Cypress) or 3 mm diameters (Bioanalytical Systems) were used as the working electrodes. These electrodes were routinely polished with a 0.3 µm alumina slurry on Microcloth polishing cloth, rinsed copiously with deionised water, sonicated in an ultrasonic bath for 5 min then washed with acetone and dried in air. For the bulk electrolysis experiment, a large platinum basket was used as the working electrode. Depending on the solvent/electrolyte media, the reference electrode was either Ag/AgCl, separated from the analyte solution by a fine frit containing the same solvent/supporting electrolyte mixture, or a BAS aqueous Ag/AgCl (3 M KCl). The counter electrode was made from platinum mesh. Analyte solutions of $\sim10^{-3}$ M were prepared in dichloromethane containing: 0.1 M tetrabutylammonium hexafluorophosphate ($[NBu_4][PF_6]$), 0.05 M tetrabutylammonium *tetrakis*(pentafluorophenyl)borate ($[NBu_4][B(C_6F_5)_4]$), or 0.33 M or 0.2 M 1-butyl-1-methylpyrrolidinium bis(trifluoromethylsulfonyl)amide ([bmpyr][TFSA]) as the supporting electrolyte. All potentials measured in CH_2Cl_2/electrolyte media are referenced to the reversible formal potential (taken as $E^{\circ\prime}=0.000$ V) for the decamethylferricenium/decamethylferrocene ($Fc^{*+/0}$) couple [25], where $E^{\circ\prime}$

Fig. 1 Monomer, polymer and electrolyte structures
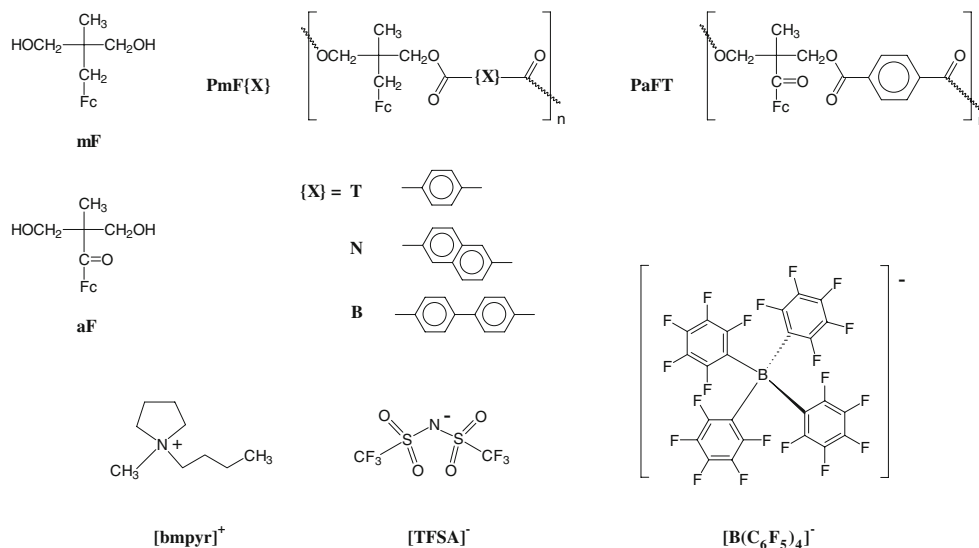
was calculated from the average of the oxidation and reduction peak potentials under conditions of cyclic voltammetry. Under these conditions, $E^{o\prime}$ calculated for the $Fc^{+/0}$ process (Fc = ferrocene) was 0.55 V vs $Fc^{*+/0}$ (in CH_2Cl_2/0.1 M $[NBu_4][PF_6]$ medium) or 0.61 V (in CH_2Cl_2/0.1 M $[NBu_4][B(C_6F_5)_4]$ medium) [22]. For voltammetric experiments with solids, ferrocenyl polyesters were immobilised onto the working electrode surface via mechanical attachment (small amount of the solid was transferred to a piece of weighing paper over which the electrode was rubbed, thus causing the solid to adhere to the surface). UV–visible spectra of bulk electrolysis solutions and product were recorded with a Varian Cary 5000 UV–vis spectrophotometer using a 1-mm path length quartz cuvette. Band maxima were obtained from convoluted spectra.

Results and discussion

Synthesis and properties of the polymers

The synthesis of the ferrocenyl-*neo*-pentylenediol monomers **mF** and **aF** (Fig. 1) has previously been described [23]. These are yellow and orange crystalline solids, respectively, with good solubility and stability in chlorinated, aromatic and polar organic solvents. Their behaviour across the full range of the electronic, vibrational and nuclear magnetic spectrum is typical of alkyl (**mF**) and acyl (**aF**) ferrocenes.

The polyesters were synthesised [24] utilising the carbodiimide-based coupling method of Moore and Stupp [26]. Following this protocol, the diol monomer **mF** was reacted with a series of aromatic dicarboxylic acids to form polyesters with a pendant ferrocenyl group **PmF{X}** in good yield: **{X}** = **T**, terephthalate; **N**, 2,6-naphthalene dicarboxylate; **B**, 4,4′-biphenyl dicarboxylate. The mild conditions also allowed the successful polymerisation of the acyl diol monomer **aF** with terephthalic acid to give **PaFT**. The resulting polymers were soluble in toluene and halogenated solvents, but insoluble in MeCN, acetone and simple alcohols. Their colour, yellow (**PmF{X}**) and orange (**PaFT**), reflects their derivation from the yellow **mF** or orange **aF** monomers respectively. Spectroscopic properties (NMR, IR and electronic) appear as a superposition of the components of the aromatic carboxylate and the methyl- or acylferrocenyl monomer precursor.

The molecular weights obtained for the polymers are not high; the typical number average chain length (or ring system) equates to 11 repeat units. Unlike random or block co-polymers and independent of the chain length, a design feature of these polyesters is the regular spacing of the ferrocenyl unit, one per repeat unit, through the polymer chains. This has two important consequences. The first is

that it provides for direct comparison between monomer and 'per repeat unit' polymer properties. As an example, for the methylferrocenyl polymers (**PmF{X}**), the low energy ferrocenyl d–d band is observed at λ_{max} 438 nm with an extinction coefficient calculated on a per repeat unit basis of $\varepsilon \sim 110$ $mol^{-1}cm^{-1}$ dm^3, directly comparable with their **mF** monomer precursor (λ_{max} 442 nm, $\varepsilon=130$). The second consequence of the polymer regularity is that it enables a reliable estimation of the electroactive groups per mass, irrespective of individual polymer chain lengths. This property was exploited in the stoichiometric per repeat unit 2,3-dichloro-5,6-dicyanoquinone (DDQ) oxidation of the pendant ferrocenyl groups of **PmFT** [24] and allows electrochemical measurements to be undertaken in this paper on solutions of a known concentration of electroactive material. Similar assumptions have been made previously in an analysis of poly(vinylferrocene) electrochemistry [12].

We have previously reported the chemical oxidation of a CH_2Cl_2 solution of **PmFT** with DDQ added in a stoichiometric per repeat unit equivalent to prepare polymer chains of the composition $[PmFT]^{nt}([DDQ]^{\bullet-})_n$ [24]. The oxidation was accompanied by a colour change to red-brown, which is the result of strong absorptions in the visible region of the UV–visible spectrum, 346–589 nm, a signature associated with the $[DDQ]^{\bullet-}$ radical anion [27]. Although these data provided direct evidence of DDQ reduction, the corresponding evidence for ferrocenyl group oxidation, a decrease in the intensity of the 438 nm d–d band and appearance of a new weak ligand-to-metal charge transfer (LMCT) band at 630 nm, is totally masked by the order of magnitude larger $[DDQ]^{\bullet-}$ absorption.

The oxidised species $[PmFT]^{nt}([DDQ]^{\bullet-})_n$ is markedly less soluble in CH_2Cl_2 than the neutral polymer **PmFT**, but solubility in the polar solvents MeCN and MeOH is greatly enhanced. These dramatic differences in solubility between neutral and oxidised polymer forms provide a difficulty in achieving ideal solution-based electrochemical behaviour as discussed below.

Solution-phase electrochemistry

The results of voltammetric oxidation of monomers **mF** and **aF** and ferrocenyl polyesters **PmF{X}** and **PaFT** in dichloromethane are summarised in Table 1. Cyclic voltammetry of the monomers (**mF** and **aF**) exhibited the expected reversible one electron oxidation process associated with the ferrocenyl group. The reversible formal potential (E^{o}) values for these fully solution-phase processes in a traditional 0.1 M $[NBu_4]$ $[PF_6]/CH_2Cl_2$ electrolyte medium occurred at 0.49 and 0.77 V, respectively, vs Fc* and are consistent with literature values for alkyl- and acylferrocenyls [28, 29].

For the polymers, the use of the traditional $[PF_6]^-$ supporting electrolyte anion and low-polarity dichloro-

Table 1 Reversible potentials for monomers and polymers in dichloromethane containing different supporting electrolytes

Analyte	$E^{o\prime}/V$ [a]		
	$[PF_6]^-$ [b]	$[B(C_6F_5)_4]^-$ [c]	$[TFSA]^-$ [d]
mF	0.49	0.57	
aF	0.77	0.84	
PmFT	0.52[e]	0.61	0.56[e]
PmFN	0.55[e]	0.62	
PmFB	0.53[e]	0.62	
PaFT	0.79[e]	0.90	
Ferrocene [f]	0.55	0.61	

[a] All potentials measured vs Fc* internal reference

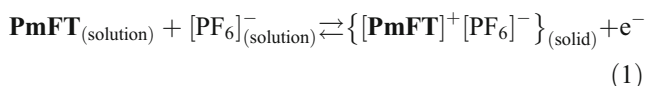[b] CH_2Cl_2/0.1 M $[NBu_4][PF_6]$

[c] CH_2Cl_2/0.05 M $[NBu_4][B(C_6F_5)_4]$

[d] CH_2Cl_2/0.33 M or 0.2 M [bmpyr][TFSA] gave the same $E^{o\prime}$

[e] E_m (calculated from the average of the oxidation and reduction peak potentials)

[f] Data from Ref. [22]

methane solvent produces product surface interaction phenomena (Fig. 2a), probably due to very rapid precipitation (electrocrystallisation) of the generated polymeric cationic species as the hexafluorophosphate salt ['polymer']$^{n+}[PF_6]_n$, on the electrode surface. Thus, the probable overall reaction for the ferrocenyl in one polymer repeat unit is as given in Eq. 1.

$$\mathbf{PmFT}_{(solution)} + [PF_6]^-_{(solution)} \rightleftharpoons \left\{ [\mathbf{PmFT}]^+ [PF_6]^- \right\}_{(solid)} + e^- \tag{1}$$

Reversal of the potential regenerates the soluble neutral polymer species, and repeat scans overlay almost completely. This stripping-type behaviour observed in the voltammetry of the **PmFT** polyester, as a representative example, is not unprecedented. It has been observed regularly for polycations in low-polarity solvents since the first electrochemical study of poly(vinylferrocene) [12]. In recognition of lack of diffusion control, the term mid-point (E_m) potential (calculated as the average of the oxidation and reduction peak potentials) is now reported instead of $E^{o\prime}$ for processes involving surface interactions, although the two terms are likely to have similar values. The different aromatic groups in the polyester backbone have only a minimal effect on the E_m value, but the methyl- or acyl linkage, by which the ferrocenyl group is attached, results in a circa 300 mV difference between **PmF{X}** and **PaFT** that mirrors that observed between monomers **mF** and **aF**.

Ionic liquids are attracting wide attention in fundamental electrochemical studies [30] as well as an increasing
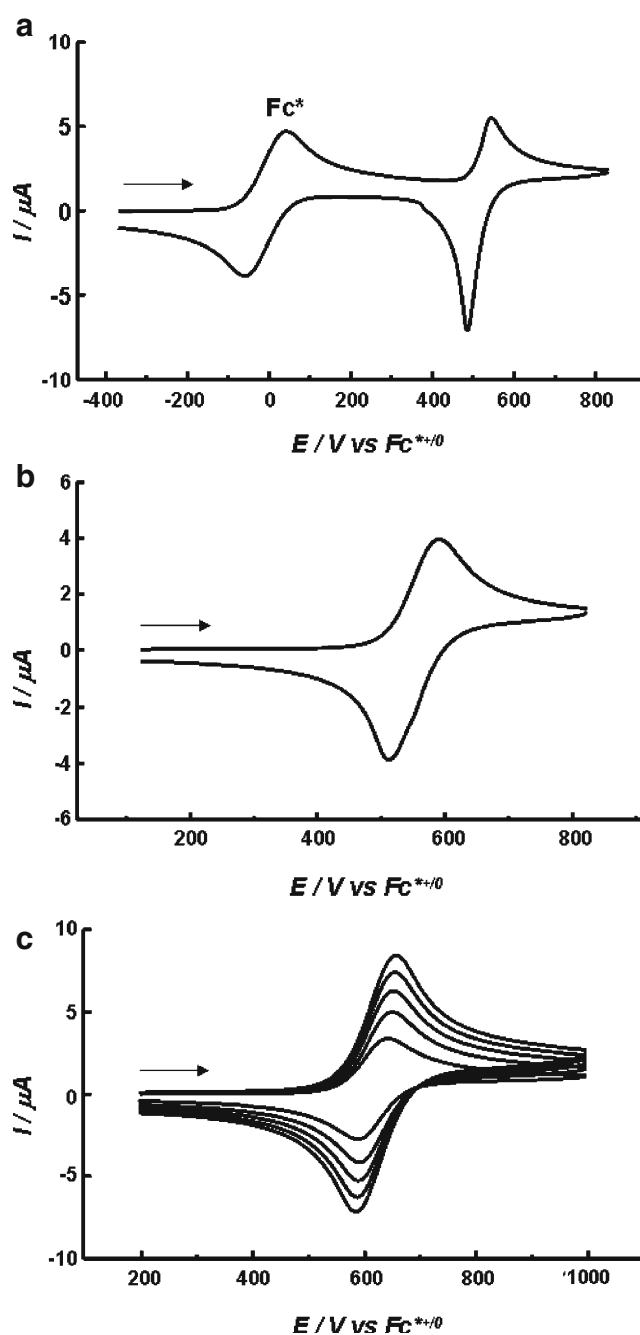
Fig. 2 Cyclic voltammograms obtained with a 1.5-mm-diameter GC electrode for oxidation of 1 mM **PmFT**: **a** CH_2Cl_2/0.1 M $[NBu_4][PF_6]$, scan rate of 100 mV s^{-1}; **b** CH_2Cl_2/0.33 M [bmpyr][TFSA], scan rate of 100 mV s^{-1}; **c** CH_2Cl_2/0.05 M $[NBu_4][B(C_6F_5)_4]$, scan rates 100–500 mV s^{-1}

number of specialist industrial applications. Following the above experiments in conventional $CH_2Cl_2/[PF_6]^-$ solutions, we examined the polymer electrochemistry with the RTIL 1-butyl-1-methylpyrrolidinium bis(trifluoromethylsulfonyl)amide ([bmpyr][TFSA]) employed as the supporting electrolyte. **PmFT** was predictably insoluble in neat [bmpyr][TFSA], but concentrations up to 0.33 M of the IL

dissolved in CH_2Cl_2 solutions allowed for dissolution of the neutral polymer. Cyclic voltammograms obtained under these conditions (Fig. 2b) show similarities with those obtained with $[NBu_4][PF_6]$ as the supporting electrolyte, i.e. a degree of surface interaction of the oxidised polymer species was detected. Equation 2 represents the overall reaction for oxidation of one ferrocenyl unit with [bmpyr] [TFSA] as the supporting electrolyte. However, in this case, the reverse or oxidative scan is less affected by the surface interaction phenomena, suggesting that although the use of the TFSA anion does not allow the precipitation of the product to be completely outrun on the voltammetric time scale used in these studies, it does allow achievement of a much closer approach to diffusion-controlled electrochemical behaviour.

$$\mathbf{PmFT}_{(solution)} + [TFSA]^-_{(solution)} \rightleftarrows \left\{[\mathbf{PmFT}]^+[TFSA]^-\right\}_{(solid)} + e^- \tag{2}$$
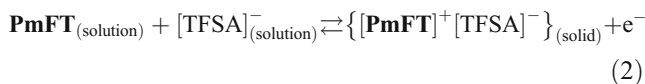
The large and lipophilic fluoroaryl borate anion $[B(C_6F_5)_4]^-$ has been shown to stabilise reactive cations and unusual dimer radicals of transition metals [19, 20]. Importantly, for the purposes of this work, the much weaker interaction of this weakly coordinating anion proved to be advantageous [21]. Thus, in a marked contrast to the surface interaction (precipitation or adsorption) encountered with other electrolytes, essentially ideal diffusion-controlled behaviour was observed when $[B(C_6F_5)_4]^-$ was used as the supporting electrolyte anion. In CH_2Cl_2/0.05 M $[NBu_4][B(C_6F_5)_4]$, all the studied polyester compounds gave rise to a single one electron chemically and electrochemically reversible oxidation process (Fig. 2c). Peak-to-peak separations (E_{pox}–E_{pred}) were 60–70 mV at slow scan rates, very similar to the values measured, in this work, for both ferrocene and decamethylferrocene under the same conditions, and importantly, close to the value of 57 mV predicted for a polymer with multiple non-interacting redox centres [13]. The chemical reversibility of these polyester systems were established by reference to the usual diagnostic criteria available in cyclic voltammetry (oxidation and reduction peak heights being equal in magnitude, i.e. current ratio equals unity over the entire scan rate range (100 to 1,000 mV s^{-1}) and double potential step chronoamperometry (step time 1–5 s; $i_r(2\tau)/i_f(\tau)$=0.25–0.28, which is close to experimental value of 0.27 recorded for the Fc$^{0/+}$ couple in same medium) [19]. Values of $E^{o\prime}$ (referenced to internal Fc*) obtained with $[NBu_4][B(C_6F_5)_4]$ supporting electrolyte differ significantly from E_m values in $[NBu_4][PF_6]$ (see Table 1), but show a similar variation to that observed for the ferrocene molecule in the two supporting electrolytes [22]. Again, the aromatic groups of the polyester spine have a negligible effect on the $E^{o\prime}$ value, whereas the pendant

methyl- or acylferrocenyl groups produce an approximately 300 mV difference between $\mathbf{PmF\{X\}}$ and $\mathbf{PaFT}$.

On the basis of the rapid and readily detected surface interaction of $[\mathbf{PmFT}]^+$ in media containing either $[PF_6]^-$ or $[TFSA]^-$ anions, the possible weak surface activity of $[\mathbf{PmFT}][B(C_6F_5)_4]$ with $[B(C_6F_5)_4]^-$ as the electrolyte anion was examined by performing double potential step chronocoulometric measurements as a function of step time (0.5 to 10 s). Anson plots constructed from these data (Fig. 3) clearly establish the absence of surface interaction for both the neutral polyester starting material and the generated cationic species, thereby confirming the diffusion-controlled nature of the redox processes associated with the polyester compounds in the presence of $[B(C_6F_5)_4]^-$ anion. Equation 3 represents the overall reaction detected on the voltammetric timescale for oxidation of one ferrocenyl unit under these conditions. Presumably, the product is soluble or the kinetics of precipitation of polymeric $[\mathbf{PmFT}][B(C_6F_5)_4]$ when $[NBu_4][B(C_6F_5)_4]$ is the supporting electrolyte are too slow to be detected on the time scale of the cyclic voltammetric or double potential step experiments.

$$\mathbf{PmFT}_{(solution)} + [B(C_6F_5)_4]^-_{(solution)} \rightleftarrows [\mathbf{PmFT}]^+[B(C_6F_5)_4]^-_{(solution)} + e^- \tag{3}$$
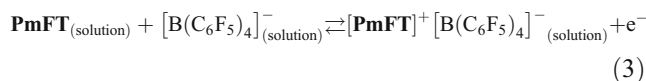
The diffusion coefficients (D) of these compounds (Table 2) were determined from the slopes of peak current (i_p) vs the square root of the scan rate ($v^{1/2}$) plots derived from the oxidation component of cyclic voltammograms
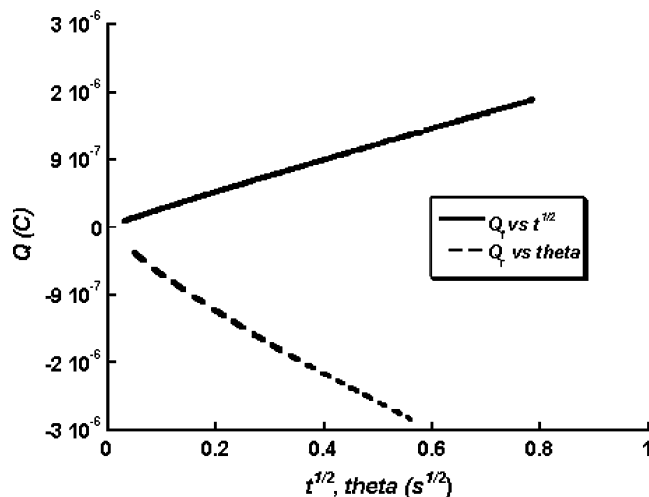
Fig. 3 Anson plot obtained for the oxidation of 1 mM $\mathbf{PmFT}$ in CH_2Cl_2/0.05 M $[NBu_4][B(C_6F_5)_4]$ at a 1.5-mm-diameter GC disk electrode using a step time of 1 s. In this figure, Q_f is the charge associated with the oxidation step, Q_r is the charge associated with the reduction counterpart, t is the step time, τ is the duration time, and theta $= \tau^{1/2} + (t-\tau)^{1/2} - t^{1/2}$

Table 2 Diffusion coefficient (D) in CH_2Cl_2 of monomers and polymers

	$D/cm^2\ s^{-1}$		M_w	Calc.[a] $D_o/cm^2\ s^{-1}$
	$[PF_6]^{-\ b}$	$[B(C_6F_5)_4]^{-\ c}$		
mF	1.3×10^{-5}	1.1×10^{-5}	288	
aF	9.6×10^{-6}	9.2×10^{-6}	302	
PmFT	–	5.5×10^{-6}	$4,500^{d}$	2.4×10^{-6}
PmFN	–	7.0×10^{-6}	$5,400^{d}$	2.2×10^{-6}
PmFB	–	3.6×10^{-6}	$6,600^{d}$	2.0×10^{-6}
PaFT	–	5.2×10^{-6}	$4,000^{d}$	2.2×10^{-6}
Ferrocene	$1.67 \times 10^{-5\ e}$	$2.1 \times 10^{-5\ g}$	186	
Fc*	$1.3 \times 10^{-5\ f}$	$1.5 \times 10^{-5\ g}$	326	

[a] Calculated from Eq. 5

[b] 0.1 M $[NBu_4][PF_6]/CH_2Cl_2$

[c] 0.05 M $[NBu_4][B(C_6F_5)_4]/CH_2Cl_2$

[d] Number average molecular weight (M_n) determined by gel permeation chromatography [24]

[e] Data (298 K) from Ref. [36]

[f] Data (298 K) from Ref. [37]

[g] 0.1 M $[NBu_4][B(C_6F_5)_4]/CH_2Cl_2$

and use of the Randles–Sevcik equation [31]. At 293 K, this can be written in a concise form as Eq. 4.

$$i_p = (2.71 \times 10^5) n^{3/2} A D^{1/2} C v^{1/2} \quad (4)$$

i_p peak current

n number of electrons transferred

A area of the electrode

D diffusion coefficient

C concentration of electroactive species

V scan rate

In this treatment, we make the assumption that the individual redox sites on the polymer are non-interacting electronically, and secondly, we ignore the physical bonds within the polymer chains, i.e. $n=1$ for the oxidation of polymer repeat units of concentration C. This treatment has been shown to be appropriate for poly(vinylferrocene) [13] and ferrocenyl substituted phosphazene polymers [14].

Also shown in Table 2 are the diffusion coefficients calculated from Eq. 5 [13, 32].

$$D_p/D_m = (M_m/M_p)^{0.55} \quad (5)$$

D_p and D_m diffusion coefficient of polymer and monomer, respectively

M_p and M_m molecular weight of polymer and monomer, respectively

The number average molecular weight (M_n) determined by gel permeation chromatography was used for M_p. Bearing in mind that the single numerical value for M_n disguises our experimental observation of a distinctive bimodal distribution in the polymer weights [24], there is reasonable agreement between the diffusion coefficients obtained experimentally and those calculated from Eq. 5.

Bulk electrolysis of **PmFT**

In the case of DDQ chemical oxidation, the ferrocenium LMCT band was obscured by strong $[DDQ]^{-}$ absorption. A bulk electrolysis experiment utilising the optically transparent hexafluorophosphate counter-anion therefore provided the opportunity to probe the visible spectrum of the oxidised polymer for evidence of this ferrocenium defining feature in the absence of the $[DDQ]^{-}$ absorption. The coulomb count recorded upon application of a potential of 0.6 V to a dichloromethane solution of **PmFT** (10 mM) was consistent with a one electron oxidation of the polymer repeat units. The visible observation of a blue/greening of the yellow polymer solution was confirmed by examination of the visible spectrum (Fig. 4) before, during and after the bulk electrolysis process. This provided evidence for oxidation of the pendant ferrocenyl groups, the spectrum during the course of oxidation showing a progressive decrease in the ferrocenyl d–d absorption at 438 nm, and appearance of a new band at 630 nm assigned to the ferrocenium LMCT band. Formation of a dark blue precipitate at the working electrode was also detected. A small sample of the dark blue precipitated $[\mathbf{PmFT}][PF_6]$ redissolved in acetone also

Fig. 4 Visible spectra of 0.01 M **PmFT** in CH_2Cl_2/ 0.1 M [NBu4][PF_6] before oxidation (*dashed line*), a 50% electrochemically oxidised solution (*dotted line*) and an acetone solution of the oxidised product precipitated from oxidation in CH_2Cl_2 (*solid line*)
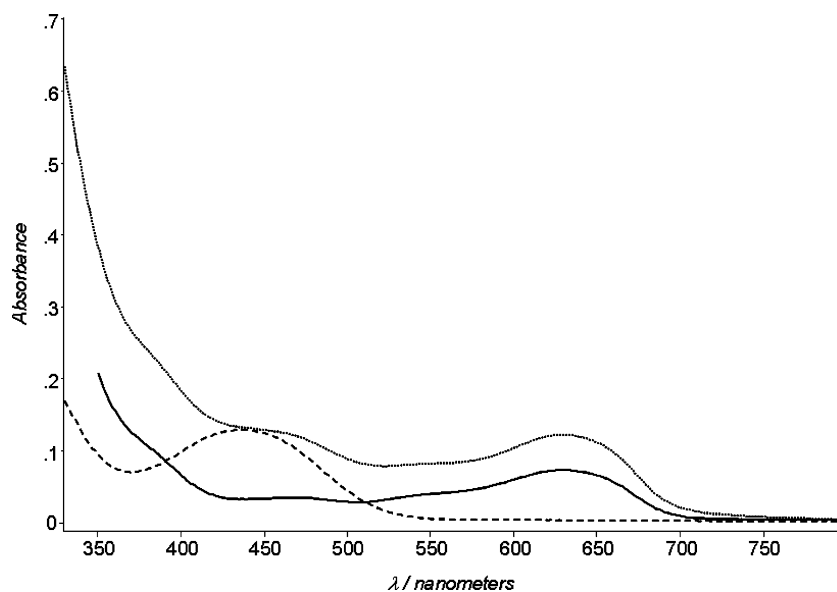
exhibited a band at 630 nm. An attempt to isolate a significant quantity of the dark blue precipitate was made by filtering off the supernatant liquid from the electrolysis solution, combining this with the acetone redissolved washings of the working electrode, and removal of the solvent under vacuum. The product proved unstable to this work-up regimen, and attempts at further characterisation were unsuccessful.

Solid-state electrochemistry of **PmFT**

Taking advantage of the poor solubility of the **PmF[X]** family of polyester compounds in aqueous and neat ionic liquid media, we have explored the redox chemistry derived from mechanically attaching microcrystals to an electrode surface. In this way, it is possible to gain insights into the factors that govern the charge transport and ion incorporation processes that take place upon oxidation of **PmFT** solid. Figure 5a displays cyclic voltammograms obtained when a **PmFT**-modified GC electrode in contact with neat [bmpyr][TFSA] ionic liquid is exposed to potential cycling over the range from 0 to 550 mV. The voltammograms again exhibit well-defined oxidation and reduction processes. However, in this case, the peak shapes are symmetrical and hence different from those obtained for dissolved species. These peaks correspond to the reversible redox reaction of the $Fc^{0/+}$ couple in the **PmFT** polyester. Although the shape approximates that expected for a surface-confined reversible one electron-transfer process, the peak-to-peak separation (E_{pox}–E_{pred}) between the oxidation and reduction components, ca. 25 mV at a scan rate of 100 mV s^{-1}, is slightly larger than the predicted value of 0 mV for an ideal reversible thin film model [31]. Furthermore, the peak width at half height ($W_{1/2}$=100 mV),
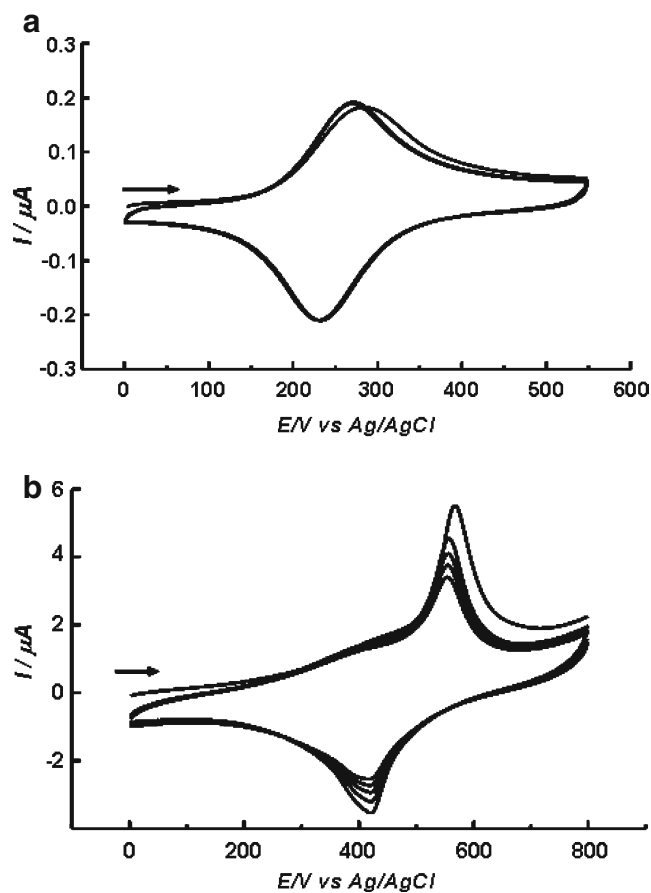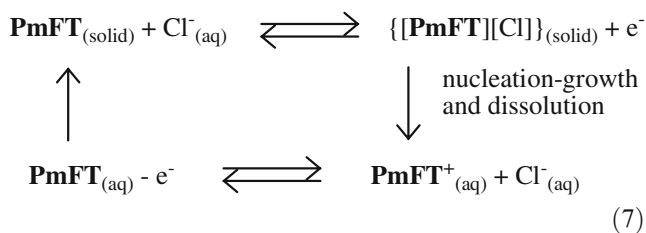
Fig. 5 Cyclic voltammograms obtained at scan rate of 100 mV s^{-1} when a 1.5-mm-diameter GC electrode containing mechanically attached **PmFT** microcrystals is placed in contact with **a** neat solution of [bmpyr][TFSA] ionic liquid and **b** an aqueous 0.1 M KCl electrolyte solution

deviates slightly from the theoretical value of 89.1 mV. These non-idealities may be attributed to ohmic effects that arise from uncompensated resistance or to kinetic or thermodynamic dispersion. Nonetheless, these observations clearly indicate that the **PmFT**$^{0/+}$ redox process occurs without dissolution of either neutral **PmFT** or the oxidised **PmFT**$^+$ species when the modified electrode is in contact with neat [bmpyr][TFSA]. Thus, the oxidation of adhered microcrystals of **PmFT** in contact with ionic liquid, again for one ferrocenyl unit, can be simply represented by Eq. 6.

$$\mathbf{PmFT}_{(solid)} + [TFSA]^-_{(ionic\,liquid)} \rightleftharpoons \left\{ [\mathbf{PmFT}]^+ [TFSA]^- \right\}_{(solid)} + e^-$$

(6)
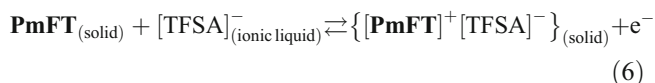
According to this postulated reaction mechanism, the oxidation process is accompanied by the ingress of TFSA$^-$ anions into the **PmFT** solid to achieve charge neutralisation, followed by their egress upon reduction.

Cyclic voltammetric responses obtained when a **PmFT**-modified GC electrode is immersed in aqueous 0.1 M KCl electrolyte solution exhibited different shapes than those obtained upon contact with ionic liquid or with solution-phase (dichloromethane) voltammetry. As shown in Fig. 5b, well-defined and sharp oxidation and reduction peaks, having a mid-point potential of 540 mV vs Ag⎮AgCl⎮3 M KCl, are detected in the first cycle of the potential. The large peak-to-peak separation (138 mV) between the oxidation and reduction components is as expected for a process governed by nucleation/growth kinetics [33–35]. Unlike the case with [bmpyr][TFSA], extensive cycling of the potential (Fig. 5b) over the range from 0 to 800 mV resulted in a progressive decrease in the peak current heights for both the oxidation and reduction processes. This is most likely caused by slow dissolution of **PmFT** microcrystals and/or oxidised [**PmFT**]$^+$ cations into the aqueous electrolyte media. Thus, the oxidation of solid **PmFT** immobilised onto GC electrode and placed in contact with aqueous 0.1 M KCl electrolyte solution is probably governed by nucleation–growth and dissolution at the GC$_{(s)}$⎮**PmFT**$_{(s)}$⎮KCl$_{(aq)}$ triple phase junction as represented by the reaction scheme given in Eq. 7, for one ferrocenyl unit. According to this mechanism, Cl$^-$ anions are incorporated into the crystal lattice when **PmFT** is oxidised and expelled on reduction of [**PmFT**]$^+$, so that chemically reversible ion transport across the solvent (electrolyte) boundary provides the conditions required for charge neutralisation.

$$\mathbf{PmFT}_{(solid)} + Cl^-_{(aq)} \rightleftharpoons \left\{ [\mathbf{PmFT}][Cl] \right\}_{(solid)} + e^-$$

nucleation-growth and dissolution

$$\mathbf{PmFT}_{(aq)} - e^- \rightleftharpoons \mathbf{PmFT}^+_{(aq)} + Cl^-_{(aq)}$$

(7)

Conclusions

Solution and solid-phase voltammetric studies on a family of ferrocenyl polyesters have shown that the one electron oxidation of the ferrocenyl groups is strongly affected by the nature of the supporting electrolyte anion. Use of the low-polarity solvent CH$_2$Cl$_2$ in the presence of traditional PF$_6^-$ as supporting electrolyte anions resulted in severe surface interaction (product precipitation and/or adsorption) problems, owing to the limited solubility of the generated polymeric cationic products in this electrolyte media. A partial solution was obtained using a CH$_2$Cl$_2$/ionic liquid combination (TFSA$^-$ as counter anions). The problem was finally overcome by replacing these anions by the large and weakly coordinating [B(C$_6$F$_5$)$_4$]$^-$, thereby leading to diffusion-controlled, chemically and electrochemically reversible processes, consistent with formation of soluble ferrocenyl-based products. Under these ideal conditions, it is evident that the acyl or methyl linkers through which the ferrocenyl group is attached to the *neo*-pentylenediol component strongly tune the reversible redox potentials of the polymers. Results obtained for the oxidation of microcrystalline **PmFT** mechanically attached to GC electrode and placed in contact with neat ionic liquid or 0.1 M KCl aqueous solution exhibit surface-confined oxidation processes, which depend upon the nature of the solvent/electrolyte media and how the ion transport across the solid⎮solid⎮solution (electrolyte) three-phase junction is coupled with the electron-transfer step. The findings of this study enhance the general understanding of the mechanistic aspects associated with electron-transfer reactions of these polyester compounds in the solution and solid-state phases.

References

1. Arimoto FS, Haven AC Jr (1955) J Am Chem Soc 77:6295. doi:10.1021/ja01628a068
2. Pittman CU Jr (2005) J Inorg Organomet Polym Mater 15:33. doi:10.1007/s10904-004-2374-6
3. Manners I (2004) Synthetic metal-containing polymers. Wiley, Weinheim
4. Gonsalves KE, Chen X (1995) Synthesis and characterization of ferrocene-containing polymers. In: Togni A, Hayashi T (eds) Ferrocenes. VCH, Weinheim, pp 497–530
5. Abd-El-Aziz AS, Todd EK (2003) Coord Chem Rev 246:3. doi:10.1016/S0010-8545(03) 00107-3
6. Whittell GR, Manners I (2007) Adv Mater 19:3439. doi:10.1002/adma.200702876
7. Koide S, Yokoyama K (1999) J Electroanal Chem 468:193. doi:10.1016/S0022-0728(99) 00174-6

8. García Armada MP, Losada J, Cuadrado I, Alonso B, González B, Casado CM, Zhang J (2004) Sens Actuators, B 101:143. doi:10.1016/j.snb.2004.02.043

9. Nagel B, Warsinke A, Katterle M (2007) Langmuir 23:6807. doi:10.1021/la700331w

10. Neuse EW (2005) J Inorg Organomet Polym Mater 15:3. doi:10.1007/s10904-004-2371-9

11. Hudson RDA (2001) J Organomet Chem 637–639:47. doi:10.1016/S0022-328X(01) 01142-1

12. Smith TW, Kuder JE, Wychick D (1976) J Polym Sci 14:2433

13. Flanagan JB, Margel S, Bard AJ, Anson FC (1978) J Am Chem Soc 100:4248. doi:10.1021/ja00481a040

14. Crumbliss AL, Cooke D, Castillo J, Wisian-Neilson P (1993) Inorg Chem 32:6088. doi:10.1021/ic00078a029

15. Morikita T, Yamamoto T (2001) J Organomet Chem 637–639:809. doi:10.1016/S0022-328X(01) 00941-X

16. Casado CM, Cuadrado I, Morán M, Alonso B, García B, González B, Losada J (1999) Coord Chem Rev 185–186:53. doi:10.1016/S0010-8545(98) 00252-5

17. Gnedenko BB, Ryabov AD (1994) Anal Chem 66:2240. doi:10.1021/ac00086a007

18. Foucher DA, Honeyman CH, Nelson JM, Tang BZ, Manners I (1993) Angew Chem Int Ed Engl 32:1709. doi:10.1002/anie.199317091

19. Nafady A, Geiger WE (2008) Organometallics 27:5624. doi:10.1021/om800546d

20. Nafady A, Costa PJ, Calhorda MJ, Geiger WE (2006) J Am Chem Soc 128:16587. doi:10.1021/ja0653775

21. Camire N, Mueller-Westerhoff UT, Geiger WE (2001) J Organomet Chem 637–639:823. doi:10.1016/S0022-328X(01) 00956-1

22. Barrière F, Geiger WE (2006) J Am Chem Soc 128:3980. doi:10.1021/ja058171x

23. McAdam CJ, Moratti SC, Robinson BH, Simpson J (2008) J Organomet Chem 693:2715. doi:10.1016/j.jorganchem.2008.05.019

24. McAdam CJ, Nafady A, Bond AM, Moratti SC, Simpson J (2008) J Inorg Organomet Polym Mater 18:485. doi:10.1007/s10904-008-9228-6

25. Noviandri I, Brown KN, Fleming DS, Gulyas PT, Lay PA, Masters AF, Phillips L (1999) J Phys Chem B 103:6713. doi:10.1021/jp991381+

26. Moore JS, Stupp SI (1990) Macromolecules 23:65. doi:10.1021/ma00203a013

27. Miller JS, Krusic PJ, Dixon DA, Reiff WM, Zhang JH, Anderson EC, Epstein AJ (1986) J Am Chem Soc 108:4459. doi:10.1021/ja00275a036

28. Gan J, Tian H, Wang Z, Chen K, Hill J, Lane PA, Rahn MD, Fox AM, Bradley DDC (2002) J Organomet Chem 645:168. doi:10.1016/S0022-328X(01) 01416-4

29. McAdam CJ, Morgan JL, Robinson BH, Simpson J, Rieger PH, Rieger AL (2003) Organometallics 22:5126. doi:10.1021/om0304659

30. Trulove PC, Mantz RA (2008) Electrochemical properties of ionic liquids. In: Wasserscheid P, Welton T (eds) Ionic liquids in synthesis 1, 3rd edn. Wiley, Weinheim, pp 141–174

31. Bard AJ, Faulkner LR (2001) Electrochemical methods: fundamentals and applications. Wiley, New York

32. Tanford C (1961) The physical chemistry of macromolecules. Wiley, New York, p 362

33. Scholz F, Meyer B (1998) Voltammetry of solid microparticles immobilized on electrode surfaces. In: Bard AJ (ed) Electroanalytical chemistry, vol. 20. Marcel Dekker, New York, p 1 and references therein

34. Suárez MF, Marken F, Compton RG, Bond AM, Miao W, Raston CL (1999) J Phys Chem B 103:5637. doi:10.1021/jp990926x

35. Bond AM, Fletcher S, Marken F, Shaw FSJ, Symons PG (1996) J Chem Soc, Faraday Trans 92:3925. doi:10.1039/ft9969203925

36. Tsierkezos NG (2007) J Solution Chem 36:289. doi:10.1007/s10953-006-9119-9

37. Gennett T, Milner DF, Weaver MJ (1985) J Phys Chem 89:2787. doi:10.1021/j100259a018